Ultrafine Particles Exert Prothrombotic but Not Inflammatory Effects on the Hepatic Microcirculation in Healthy Mice In Vivo

Andrej Khandoga, MD; Andreas Stampfl, MSc; Shinji Takenaka, DVM; Holger Schulz, MD; Roman Radykewicz, BSc; Wolfgang Kreyling, PhD; Fritz Krombach, DVM

Background—Air pollution episodes are strongly associated with increased cardiovascular morbidity and mortality. The effect of ultrafine particles (UFPs), when translocated after inhalation, on the microcirculation of extrapulmonary organs remains unclear.

Methods and Results—In C57BL/6 mice, either carbon black UFPs (1×10^7 and 5×10^7) or vehicle was infused intra-arterially. Two hours after infusion, platelet– and leukocyte–endothelial cell interactions, sinusoidal perfusion, endothelial fibrin(ogen) deposition, and phagocytic activity of Kupffer cells were analyzed by intravital video fluorescence microscopy in the liver microvasculature. Expression of fibrin(ogen), von Willebrand factor (vWF), and P-selectin on hepatic endothelium was determined by immunostaining. Apoptotic cells were quantified in TUNEL-stained tissue sections. Application of UFPs caused significantly enhanced platelet accumulation on endothelium of postsinusoidal venules and sinusoids in healthy mice. UFP-induced platelet adhesion was not preceded by platelet rolling but was strongly associated with fibrin deposition and an increase in vWF expression on the endothelial surface. In contrast, inflammatory parameters such as the number of rolling/adherent leukocytes, P-selectin expression/translocation, and the number of apoptotic cells were not elevated 2 hours after UFP exposure. In addition, UFPs did not affect sinusoidal perfusion and Kupffer cell function.

Conclusions—UFPs induce platelet accumulation in the hepatic microvasculature of healthy mice that is associated with prothrombotic changes on the endothelial surface of hepatic microvessels. Accumulation of particles in the liver exerts a strong procoagulatory impact but does not trigger an inflammatory reaction and does not induce microvascular/hepatocellular tissue injury. **(*Circulation*. 2004;109:1320-1325.)**

Key Words: air pollution ■ platelets ■ leukocytes ■ fibrinogen ■ microcirculation

Epidemiological studies indicate that peaks of ambient particulate air pollution are associated with an increase in pulmonary and cardiovascular morbidity and mortality.[1,2] The involvement of the cardiovascular system was strongly supported by investigations showing an association between air concentrations of particulate matter and hospital admissions for ischemic heart disease and congestive heart failure.[3] It has been shown that exposure to particulate air pollution for as little as 2 hours increased the occurrence of myocardial infarction.[1] Moreover, air pollution episodes were associated with an increased heart rate,[4] decreased heart rate variability,[5] and elevated risk of implanted cardioverter-defibrillator discharges.[2] Although the exact mechanism by which airborne particles exert adverse effects is unknown, ambient particles are thought to enhance pulmonary inflammation associated with systemic hypercoagulability, generation of oxidants, activation of complement, increase in blood viscosity, and elevation of fibrinogen and C-reactive protein plasma concentration (reviewed by Donaldson et al[6,7]).

Recent investigations provide evidence that the smallest ultrafine particles (UFPs) can be translocated from the lungs into the circulation and extrapulmonary organs (ie, liver, heart, spleen, brain)[8–11] and therefore might potentially influence cardiovascular end points directly. Indeed, Nemmar et al[12–15] have reported that intratracheally instilled UFPs are quickly translocated into the circulation and able to activate circulating platelets and affect experimental thrombosis. Because inflammatory and prothrombotic events manifest themselves on the level of the microcirculation, it is likely that the microvasculature represents the primary target for circulating particles or particles accumulated in extrapulmonary organs. However, the microvascular effects of translocated UFPs remain as yet unknown.

Received August 14, 2003; revision received November 11, 2003; accepted November 17, 2003.

From the Institute for Surgical Research, University of Munich, Munich, Germany (A.K., F.K.); and GSF–National Research Center for Environment and Health, Institute of Toxicology (A.S., R.R.), Institute for Inhalation Biology (S.T., H.S., W.K.), and Focus Network Aerosols and Health (W.K.), Neuherberg, Germany.

Correspondence to Prof Dr Fritz Krombach, Institute for Surgical Research, University of Munich, Marchioninistraße 27, D-81377 Munich, Germany. E-mail krombach@icf.med.uni-muenchen.de

Circulation **is available at http://www.circulationaha.org** **DOI: 10.1161/01.CIR.0000118524.62298.E8**

In the present study, we investigated the impact of UFPs on the microcirculation of the liver, because it is well known that particles that are translocated in the lung accumulate predominantly in this organ.[10,11,15] Moreover, the liver plays a prominent role in metabolic (glucose homeostasis, lipoproteins), synthetic (albumin, fibrinogen, coagulation factors, complement, binding proteins), catabolic (hormones, xenobiotics), and excretory (bilirubin, cholesterol, phospholipids, copper) processes. Therefore, the intrahepatic accumulation of UFPs might potentially initiate functional disturbances, aggravating preexisting cardiovascular diseases. Consequently, we hypothesized that the intrahepatic accumulation of UFPs triggers the activation of prothrombotic pathways and induces inflammatory reactions in the liver.

Methods

Animals, Anesthesia, and Surgical Procedure

Female C57Bl/6 mice (Charles River, Sulzfeld, Germany) ranging in age from 5 to 7 weeks were used. All experiments were performed according to the German legislation on protection of animals.

The animals were anesthetized by inhalation of isoflurane–N_2O (Fi_{O_2} 0.35, 0.015 L/L isoflurane; Forene Abbott GmbH). A polyethylene catheter was inserted into the left carotid artery for recording of mean arterial blood pressure; for infusion of UFPs, fluorescent dyes, and fluorescent platelets; and for blood sampling. Two hours after infusion of UFPs, the abdominal cavity was assessed by a midline laparotomy and the left liver lobe was exteriorized for intravital microscopy.

Ultrafine Particles

We used a filtered suspension of ultrafine carbon black particles (Printex 90; diameter, 14 nm; surface area, 300 m^2/g) in 200 μL of Krebs-Henseleit buffer with 0.15% of human albumin. To minimize particle aggregation, particles were sonicated for 15 minutes and vortexed immediately before intravascular administration. The particle suspension was examined by transmission electron microscopy as described previously.[8] Approximately 60% of particles in the suspension had a diameter <100 nm. UFPs were infused into the aortic arch via the carotid artery, so that the experimental design mimics the effect of inhaled particles translocated into the pulmonary veins and the systemic circulation. The strength of this approach is that it circumvents effects related to the pulmonary accumulation of particles, eg, release of inflammatory mediators from the lung parenchyma. The estimated total number of particles infused was either 1×10^7 or 5×10^7. According to experimental and epidemiological data, this range roughly characterizes the daily amount of UFPs translocated from the lungs into the blood in mice during inhalation studies[11,16] or in humans exposed to prevailing UFP concentrations in urban air.[17,18]

Experimental Groups

Animals were randomly assigned to the following groups: (1) a control group after infusion of 200 μL of Krebs-Henseleit buffer with 0.15% albumin as a vehicle (n=6), (2) a group after infusion of 1×10^7 UFPs (n=6), and (3) a group after infusion of 5×10^7 UFPs (n=6). In an additional group (n=6), platelet–endothelial cell interactions were investigated after blockade of glycoprotein IIb/IIIa receptors on platelets with tirofiban (36 μg/g body weight,[19] Merck, Sharp and Dohme), infused intra-arterially immediately after UFP application. The exposure time after infusion of either vehicle or particles was 2 hours in all groups.

Intravital Fluorescence Microscopy

The hepatic microcirculation was analyzed by an epi-illumination technique 2 hours after infusion of either UFPs or vehicle using an intravital videofluorescence microscope (Leitz) as described previously.[20–22] For intravital microscopy, platelets were isolated from syngeneic mice and labeled ex vivo by rhodamine 6G (50 μL 0.05% per mL whole blood; Sigma-Aldrich) as described previously.[23] Two hours after application of UFPs, a total of 1×10^8 fluorescence-labeled platelets were infused intra-arterially, and platelet–endothelial cell interactions were analyzed in 5 to 7 terminal arterioles and postsinusoidal venules and in all visible sinusoids of 5 to 7 acini using an N2 filter block (excitation, 530 to 560 nm; emission, >580 nm; Leitz). Immediately thereafter, leukocyte–endothelial cell interactions were visualized within 5 to 7 postsinusoidal venules after infusion of rhodamine 6G (0.1 mL, 0.05%, Sigma-Aldrich) intra-arterially. Next, fluorescein isothiocyanate (FITC)–labeled dextran (MW 150 000; 0.1 mL, 5%, Sigma-Aldrich) was infused and liver acini were scanned using an I2/3 filter block (excitation, 450 to 490 nm; emission, >515 nm; Leitz) for assessment of sinusoidal perfusion and microvascular permeability.[20,21] Twenty minutes was required to complete intravital microscopy.

Rolling platelets and leukocytes were defined as cells crossing an imaginary perpendicular through the vessel at a velocity markedly lower than the centerline velocity in the microvessel. Their numbers are given as cells per second per vessel cross section. Platelets and leukocytes firmly attached to the endothelium for >20 seconds were counted as permanently adherent cells and expressed as number of cells per square millimeter of endothelial surface. In sinusoids, the number of accumulated platelets was counted in the scanned acini and is given in [1/acinus]. The sinusoidal perfusion rate was calculated as the percentage of perfused sinusoids per acinus.

Immunostaining for Fibrin(ogen), P-Selectin, and von Willebrand Factor

Samples of liver tissue were taken at the end of intravital microscopy (140 minutes after UFP or vehicle application). Paraffin sections (6 μm) were quenched with 0.5% H_2O_2 methanol solution to block production of endogenous peroxidase, incubated in 1.5% goat serum to block nonspecific binding, and later incubated with primary antibodies. Rabbit anti-mouse fibrinogen, von Willebrand factor (vWF), and P-selectin monoclonal antibodies (Becton Dickinson GmbH) and commercially available immunohistochemistry kits (Vectastain; Camon) were used. Control sections were incubated with an isotype-matched primary antibody. An easily detectable reddish-brown end product was obtained by development in H_2O_2/3-amino-9-ethylcarbazol. The sections were counterstained with Mayer's hemalum. In each experimental group, 6 sections from 6 individual animals (10 observation fields per section) were examined by light microscopy (magnification ×400) and analyzed semiquantitatively in a blinded manner using a grading system of 0 to 2: 0, no staining; 1, weak staining; and 2, strong staining.[20]

Plasma Fibrinogen Analysis

Plasma fibrinogen concentrations were measured by a sandwich ELISA using an IgG fraction of polyclonal goat antiserum to mouse fibrinogen for coating and a peroxidase-conjugated IgG fraction of polyclonal goat antiserum to mouse fibrinogen as conjugate (Nordic Immunology). A standard curve was generated by serial dilutions of mouse fibrinogen (Sigma-Aldrich).

Fibrin Deposition on Postischemic Hepatic Endothelium In Vivo

In a separate set of experiments, the deposition of fibrin on the endothelium of hepatic microvessels was investigated by intravital fluorescence microscopy.[20] Alexa 488–conjugated human fibrinogen (17 mg/kg; Molecular Probes) was administered intravenously before infusion of particles. To assess the microvascular distribution of fibrinogen, hepatic microvessels were scanned with an I2/3 filter block (Leitz) in animals after application of either UFPs or vehicle (n=3 each group).

In an attempt to answer the question of whether deposited fibrin was colocalized with platelet adhesion, we performed additional experiments in which rhodamine-6G–labeled platelets and Alexa-488–labeled fibrinogen were infused in the same experiment and

visualized in identical areas 2 hours after UPF infusion using 2 different filter sets.

Assessment of Apoptosis

Paraffin sections were stained by terminal deoxynucleotidyl transferase–mediated dUTP nick end-labeling (TUNEL) using a commercially available kit (Roche-Boehringer Mannheim Co). TUNEL-positive cells were counted by light microscopy (magnification ×400) in 10 high-power fields.

In Vivo Analysis of Kupffer Cell Activity

In separate experiments, the phagocytic activity of Kupffer cells was assessed by intravital fluorescence microscopy in control animals and animals after intra-arterial infusion of 5×10^7 UFPs (n=3 each group). Fifteen to 20 acini per experiment were randomly selected and visualized within 5 minutes after intra-arterial injection of 1.5×10^8/kg of plain fluorescent latex particles (diameter, 1.0 μm; Polyscience Inc) using an N2 filter block (Leitz). The kinetics of Kupffer cell activation was quantified by determining the number of particles moving in sinusoids as the percentage of all particles visible in the acini during an observation period of 10 seconds.[24,25]

Statistics

Data analysis was performed with a statistical software package (SigmaStat for Windows; Jandel Scientific). Kruskal-Wallis test and Student-Newman-Keuls test were used for the estimation of stochastic probability in intergroup comparisons. Mann-Whitney rank rum test was used for comparison of fibrinogen levels in plasma between 2 groups. Mean values±SEM are given. Probability values <0.05 were considered significant.

Results and Discussion

To analyze the impact of UFPs on the hepatic microcirculation, we used in vivo fluorescence microscopy to directly visualize and quantify interactions of blood cells with hepatic endothelium. Platelet–endothelial cell interactions were analyzed in terminal arterioles, sinusoids, and postsinusoidal venules. In the control group, almost no rolling (Figure 1A) and only a few adherent platelets (Figure 1B) were found in all types of microvessels investigated (arterioles, 40±20/mm^2; venules, 64±18/mm^2; sinusoids, 3±1/acinus). Application of UFPs increased the number of adherent platelets on endothelium of terminal arterioles (1×10^7 UFPs, 76±26/mm^2; 5×10^7 UFPs, 104±22/mm^2), but changes failed to be statistically significant.

In contrast, the number of adherent platelets in postsinusoidal venules (1×10^7 UFPs, 174±27/mm^2; 5×10^7 UFPs, 146±51/mm^2) and the number of platelets accumulated in sinusoids (1×10^7 UFPs, 8±1/acinus; 5×10^7 UFPs, 8±2/acinus) were significantly elevated after application of particles compared with the control group. Notably, UFPs predominantly initiated accumulation of single platelets in the hepatic microcirculation, whereas adhesion of platelet aggregates was only rarely detected. The extent of platelet recruitment in venules and sinusoids did not differ between the groups after application of 1×10^7 and 5×10^7 UFPs. The blockade of glycoprotein IIb/IIIa receptors, which are responsible for binding of activated platelets to fibrinogen, almost completely inhibited UFP-induced platelet adhesion. This fact suggests that the enhanced platelet accumulation on endothelium after UFP exposure is strongly associated with platelet activation and an increase in the fibrinogen-binding affinity of the glycoprotein IIb/IIIa receptor complex. Of note, platelet adhesion on the hepatic endothelium occurred without platelet rolling, because no increase in the number of rolling platelets was registered after the application of UFPs. Therefore, the character of UFP-induced platelet–endothelial cell interactions seems to be different from that of inflammation-associated interactions of platelets with the endothelium as observed in the postischemic liver in our previous investigations.[21,22,26] After hepatic ischemia-reperfusion, in contrast to UFP exposure, platelet rolling precedes permanent adhesion, and platelet adhesion is not restricted to venules and sinusoids but rather is also observed in terminal arterioles.[20]

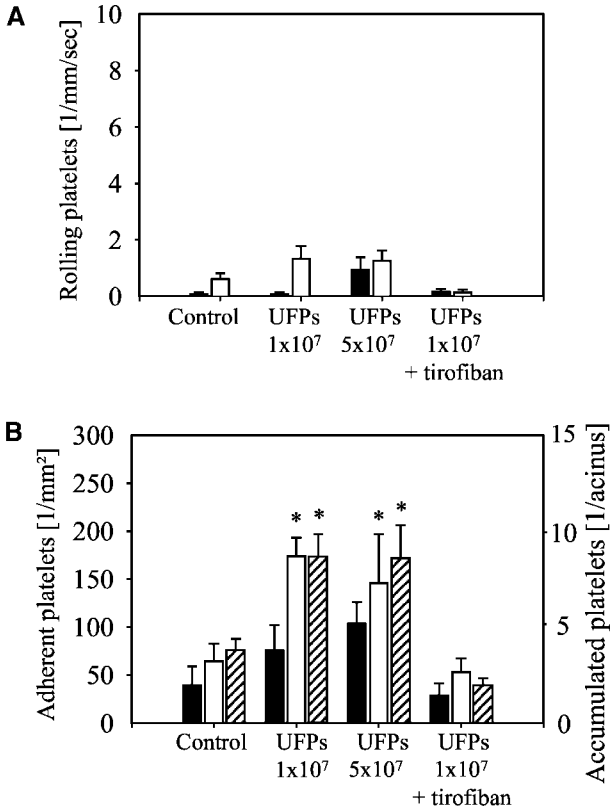

Figure 1. Numbers of rolling (A) and adherent (B) platelets in terminal arterioles (closed bars), postsinusoidal venules (open bars), and sinusoids (hatched bars) as determined by intravital microscopy. An increase in number of adherent/accumulated platelets was registered in hepatic microvessels 2 hours after intra-arterial infusion of UFPs, whereas platelet rolling remained unaffected. Glycoprotein IIb/IIIa inhibition by tirofiban almost completely attenuated platelet–endothelial cell interactions. *$P<0.05$ vs sham, n=6 each group.

Although UFPs were recently shown to enhance ADP-induced platelet activation,[14] we addressed the issue of whether platelet recruitment can be mediated by prothrombotic changes on the hepatic endothelium in response to the systemic infusion of particles. For this purpose, the intravascular distribution of fibrin(ogen) was determined in vivo using Alexa 488–conjugated fibrinogen. Under control conditions, Alexa 488–conjugated fibrinogen was found homogeneously dispersed in blood. Fibrin deposition was detectable neither in arterioles nor in sinusoids nor in postsinusoidal venules (Figure 2A). In livers of animals subjected to the UFP

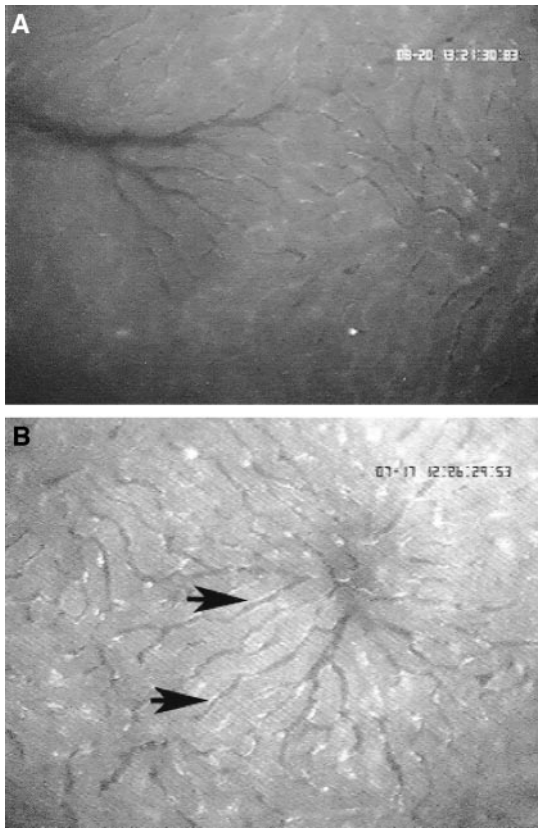

Figure 2. Intravital microscopic images demonstrating deposition of Alexa 488–conjugated fibrin(ogen) on hepatic microvascular endothelium. In control animals, no fibrin deposition was detectable (A). In contrast, fibrin bound to vascular wall in hepatic microvasculature 2 hours after application of UFPs (B, arrows).

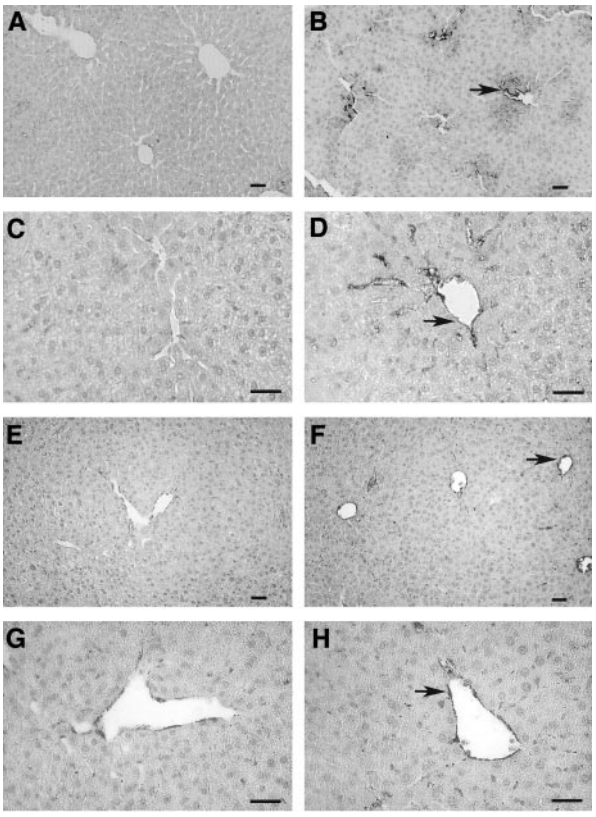

Figure 3. Immunostaining for fibrin(ogen) and vWF in hepatic microvessels of control animals (A, C and E, G, respectively) and animals after application of UFPs (B, D and F, H, respectively). Infusion of UFPs caused fibrin deposition and increased expression of vWF on hepatic endothelium (arrows). Magnification ×200 in A, B, E, and F; ×400 in C, D, G, and H. Bars=30 μm.

application, however, fluorescence-labeled fibrin was found deposited along the endothelial surface in hepatic microvessels (Figure 2B). Interestingly, ≈80% of accumulated platelets were colocalized with areas of fibrin deposition. This result supports a causal link between UFP-induced fibrin deposition and platelet accumulation. Note that we also observed fibrin deposition in heart capillaries by intravital microscopy in the same experiments (unpublished observations). This fact suggests that after UFP exposure, fibrin deposition occurs in other extrapulmonary organs as well and is not a phenomenon specific to the liver. As shown by immunohistochemistry, fibrin deposition and increased vWF expression were clearly detected on the hepatic endothelium of mice undergoing UFP application, whereas less staining was registered in control animals (Figure 3, Table).

Taken together, UFPs initiate platelet accumulation on endothelium in sinusoids and postsinusoidal venules in healthy mice that is associated with intravascular deposition of fibrin and vWF. The mechanisms that provoke platelet adhesion on hepatic endothelium and prothrombotic changes of the endothelium in response to application of UFPs remain to be clarified. The suggestion that the proadhesive effects of UFPs are triggered by systemic inflammation cannot be supported by our data on plasma levels of fibrinogen. Although the fibrinogen concentration tended to be higher after UFP application (control, 746±219 versus 10^7 UFPs, 1493±256 μg/mL), this increase did not reach statistical significance ($P=0.093$), and the values in the UFP group are still in the range of normative values in mice. Our hypothesis for future investigations is that UFPs, because of their small size, can pass through the fenestrae of sinusoidal endothelial cells (average diameter,[27] 100 nm) into the space of Disse and might increase the synthesis/release of fibrinogen and of coagulation factors on direct contact with hepatocytes.

There is a large body of evidence that particle accumulation in lungs strongly initiates an inflammatory reaction with cytokine release, oxidant generation, and activation of transcription factors for proinflammatory genes in both macrophages and epithelial cells.[7,28] It is well known from the literature and has been confirmed by our own experiments

Immunostaining for Fibrinogen, vWF, and P-Selectin

Parameter	Sham	UFP 1×10^7	UFP 5×10^7
Fibrinogen	0.4±0.2	1.2±0.1*	1.4±0.1*
vWF	0.8±0.1	1.5±0.1*	1.6±0.1*
P-selectin	0.1±0.1	0.4±0.2	0.2±0.1

Tissue sections were analyzed using a grading system of 0 to 2, as follows: 0, no staining; 1, weak staining; and 2, strong staining.

*$P<0.05$ vs sham, n=6 each group.

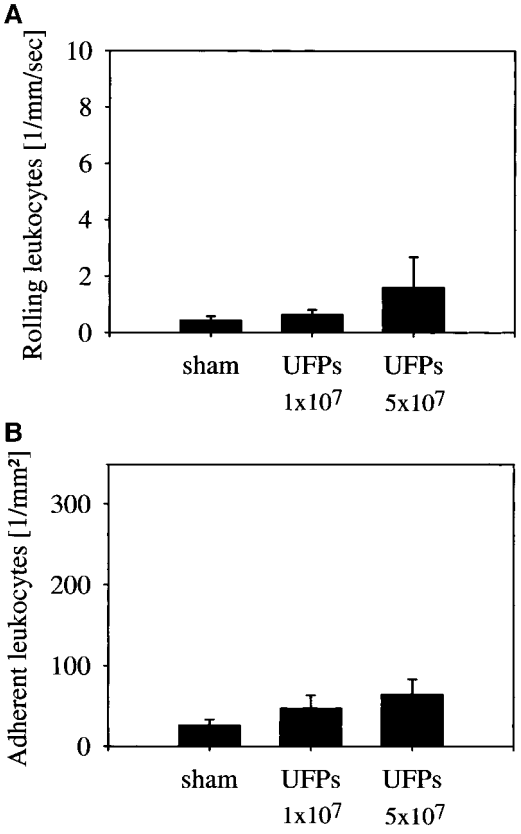

Figure 4. Numbers of rolling (A) and adherent (B) leukocytes in hepatic postsinusoidal venules as determined by intravital microscopy. No differences were observed between control group and groups after infusion of UFPs. n=6 each group.

using ultrafine insoluble radiolabeled iridium particles in the same model (Dr Kreyling, unpublished observations, 2003) that the main fraction of particles accumulates in the liver.[11,10,15] It remains unclear, however, whether this accumulation leads to an inflammatory response in the liver. Therefore, leukocyte–endothelial cell interactions were quantified in hepatic postsinusoidal venules as a parameter of the initial inflammatory reaction in the liver. In contrast to the data on platelet–endothelial cell interactions, we did not detect an increase in the extent of leukocyte–endothelial cell interactions in postsinusoidal venules of animals undergoing infusion of 1×10^7 and 5×10^7 UFPs. The numbers of both rolling (Figure 4A) and adherent (Figure 4B) leukocytes were only slightly but not significantly increased after application of UFPs compared with the control group. To support this finding, expression of the adhesion molecule P-selectin was determined on the hepatic endothelium by immunostaining. P-selectin, which is stored in granules of arteriolar/venular endothelial cells and platelets, is rapidly mobilized onto the endothelial surface on stimulation by various proinflammatory agents (ie, thrombin, histamine, oxidants) and is responsible for leukocyte and platelet rolling on hepatic endothelium.[22,29] Indeed, almost no staining for P-selectin was observed in animals subjected to UFP application followed by 2 hours of exposure (Table). This fact may explain the lack of leukocyte and platelet rolling in response to UFP exposure.

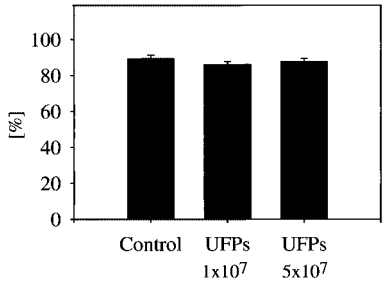

Figure 5. Sinusoidal perfusion in control group and groups after application of UFPs as determined by intravital microscopy. Sinusoidal perfusion was not affected after intra-arterial infusion of UFPs. n=6 each group.

Moreover, this supports the suggestion that UFP-induced platelet recruitment does not carry a proinflammatory character.

In an attempt to analyze whether intrahepatic accumulation of UFPs induces tissue injury, sinusoidal perfusion and apoptosis induction were determined 2 hours after intra-arterial infusion of particles. Failure of sinusoidal perfusion, which occurs because of endothelial cell swelling and hemoconcentration, is a recognized marker of microvascular injury in the liver.[30] The sinusoidal perfusion rate in the control group (89±2%) did not differ from that after infusion of UFPs (1×10^7 UFPs, 86±1%; 1×10^7 UFPs, 88±2%; Figure 5). Simultaneously with the analysis of sinusoidal perfusion, microvascular permeability to FITC-dextran was registered 2 hours after particle administration, indicating that microvascular integrity was not affected. In line with these findings, no apoptotic cells were found in livers of mice subjected to particle infusion (data not shown). From these data, it seems that intrahepatic accumulation of particles did not cause either an inflammatory reaction or cell injury in the liver. Although the reason for the quite different response of liver tissue versus lung tissue on particle accumulation remains to be elucidated, our intravital microscopic data on the phagocytic activity of Kupffer cells provide a possible explanation. In lungs, UFPs are captured by alveolar macrophages and initiate inflammation, at least in part, by impairing alveolar macrophage phagocytosis and stimulating the release of inflammatory mediators from macrophages.[28,31,32] In the liver, however, the phagocytic activity of resident macrophages (Kupffer cells), ie, the kinetics of clearance of fluorescence-labeled circulating latex particles, was found to be comparable between the groups after infusion of either 5×10^7 UFPs or vehicle, with 56±10% versus 58±1% moving particles at 1 minute, 38±7% versus 25±8% at 3 minutes, and 10±1% versus 17±4% at 5 minutes. This finding suggests that the accumulation of UFPs in the liver does not affect Kupffer cell function.

In conclusion, we show here for the first time that ultrafine carbon particles induce platelet accumulation in the hepatic microvasculature of healthy mice that is associated with prothrombotic changes on the endothelial surface of hepatic microvessels. Our findings indicate that accumulation of particles in the liver exerts a strong procoagulatory impact but does not trigger an inflammatory reaction and does not induce

microvascular/hepatocellular tissue injury. These in vivo data extend our knowledge about potential extrapulmonary effects of ultrafine ambient particles.

Acknowledgments

This study was supported by the Deutsche Forschungsgemeinschaft (FOR 440). The authors thank C. Csapo, H. Ferron, and A. Schropp for technical assistance.

References

1. Peters A, Dockery DW, Muller JE, et al. Increased particulate air pollution and the triggering of myocardial infarction. *Circulation*. 2001;103: 2810–2815.
2. Peters A, Liu E, Verrier RL, et al. Air pollution and incidence of cardiac arrhythmia. *Epidemiology*. 2000;11:11–17.
3. Schwartz J, Morris R. Air pollution and hospital admissions for cardiovascular disease in Detroit, Michigan. *Am J Epidemiol*. 1995;142:23–35.
4. Peters A, Perz S, Doring A, et al. Increases in heart rate during an air pollution episode. *Am J Epidemiol*. 1999;150:1094–1098.
5. Pope CA III, Verrier RL, Lovett EG, et al. Heart rate variability associated with particulate air pollution. *Am Heart J*. 1999;138:890–899.
6. Donaldson K, Stone V, Seaton A, et al. Ambient particle inhalation and the cardiovascular system: potential mechanisms. *Environ Health Perspect*. 2001;109(suppl 4):523–527.
7. Donaldson K, Stone V, Borm PJ, et al. Oxidative stress and calcium signaling in the adverse effects of environmental particles (PM(10)). *Free Radic Biol Med*. 2003;34:1369–1382.
8. Takenaka S, Karg E, Roth C, et al. Pulmonary and systemic distribution of inhaled ultrafine silver particles in rats. *Environ Health Perspect*. 2001;109(suppl 4):547–551.
9. Oberdorster G, Sharp Z, Atudorei V, et al. Extrapulmonary translocation of ultrafine carbon particles following whole-body inhalation exposure of rats. *J Toxicol Environ Health A*. 2002;65:1531–1543.
10. Nemmar A, Vanbilloen H, Hoylaerts MF, et al. Passage of intratracheally instilled ultrafine particles from the lung into the systemic circulation in hamster. *Am J Respir Crit Care Med*. 2001;164:1665–1668.
11. Kreyling WG, Semmler M, Erbe F, et al. Translocation of ultrafine insoluble iridium particles from lung epithelium to extrapulmonary organs is size dependent but very low. *J Toxicol Environ Health A*. 2002;65:1513–1530.
12. Nemmar A, Hoylaerts MF, Hoet PH, et al. Size effect of intratracheally instilled particles on pulmonary inflammation and vascular thrombosis. *Toxicol Appl Pharmacol*. 2003;186:38–45.
13. Nemmar A, Hoet PH, Dinsdale D, et al. Diesel exhaust particles in lung acutely enhance experimental peripheral thrombosis. *Circulation*. 2003; 107:1202–1208.
14. Nemmar A, Hoylaerts MF, Hoet PH, et al. Ultrafine particles affect experimental thrombosis in an in vivo hamster model. *Am J Respir Crit Care Med*. 2002;166:998–1004.
15. Nemmar A, Hoet PH, Vanquickenborne B, et al. Passage of inhaled particles into the blood circulation in humans. *Circulation*. 2002;105: 411–414.
16. Schulz H, Knoch C, Ritter B, et al. Does preexisting lung inflammation enhance the effects of ultrafine carbon particle exposure? In: Heinrich U, Mohr U, eds. *Crucial Issues in Inhalation Research: Mechanistic, Clinical and Epidemiologic*. Stuttgart: Frauenhofer IRB Verlag; 2002: 233–239.
17. Daigle CC, Chalupa DC, Gibb FR, et al. Ultrafine particle deposition in humans during rest and exercise. *Inhal Toxicol*. 2003;15:539–552.
18. Tuch T, Brand P, Wichmann HE, et al. Variation of particle number and mass concentration in various size ranges of ambient aerosols in Eastern Germany. *Atmos Environ*. 1997;31:4193–4197.
19. Kupatt C, Wichels R, Horstkotte J, et al. Molecular mechanisms of platelet-mediated leukocyte recruitment during myocardial reperfusion. *J Leukoc Biol*. 2002;72:455–461.
20. Khandoga A, Biberthaler P, Enders G, et al. Platelet adhesion mediated by fibrinogen-intercellular adhesion molecule-1 binding induces tissue injury in the postischemic liver in vivo. *Transplantation*. 2002;74: 681–688.
21. Khandoga A, Enders G, Biberthaler P, et al. Poly(ADP-ribose) polymerase triggers the microvascular mechanisms of hepatic ischemia-reperfusion injury. *Am J Physiol*. 2002;283:G553–G560.
22. Khandoga A, Biberthaler P, Enders G, et al. P-selectin mediates platelet-endothelial cell interactions and reperfusion injury in the mouse liver in vivo. *Shock*. 2002;18:529–535.
23. Massberg S, Enders G, Leiderer R, et al. Platelet-endothelial cell interactions during ischemia/reperfusion: the role of P-selectin. *Blood*. 1998; 92:507–515.
24. Post S, Gonzalez AP, Palma P, et al. Assessment of hepatic phagocytic activity by in vivo microscopy after liver transplantation in the rat. *Hepatology*. 1992;16:803–809.
25. Wanner GA, Mica L, Wanner-Schmid E, et al. Inhibition of caspase activity prevents CD95-mediated hepatic microvascular perfusion failure and restores Kupffer cell clearance capacity. *FASEB J*. 1999;13: 1239–1248.
26. Khandoga A, Biberthaler P, Messmer K, et al. Platelet-endothelial cell interactions during hepatic ischemia-reperfusion in vivo: a systematic analysis. *Microvasc Res*. 2003;65:71–77.
27. Steffan AM, Gendrault JL, Kirn A. Increase in the number of fenestrae in mouse endothelial liver cells by altering the cytoskeleton with cytochalasin B. *Hepatology*. 1987;7:1230–1238.
28. Donaldson K, Tran CL. Inflammation caused by particles and fibers. *Inhal Toxicol*. 2002;14:5–27.
29. Geng JG, Bevilacqua MP, Moore KL, et al. Rapid neutrophil adhesion to activated endothelium mediated by GMP-140. *Nature*. 1990;343: 757–760.
30. Vollmar B, Glasz J, Leiderer R, et al. Hepatic microcirculatory perfusion failure is a determinant of liver dysfunction in warm ischemia-reperfusion. *Am J Pathol*. 1994;145:1421–1431.
31. Renwick LC, Donaldson K, Clouter A. Impairment of alveolar macrophage phagocytosis by ultrafine particles. *Toxicol Appl Pharmacol*. 2001; 172:119–127.
32. Lundborg M, Johard U, Lastbom L, et al. Human alveolar macrophage phagocytic function is impaired by aggregates of ultrafine carbon particles. *Environ Res*. 2001;86:244–253.